

# Supernovae within the CFHLS

14 September 2001

P. Antilogus<sup>a</sup>, P. Astier<sup>b</sup>, C. Balland<sup>d</sup>, S. Basa<sup>e</sup>,  
A. Bonissent<sup>e</sup>, A. Ealet<sup>e</sup>, S. Fabbro<sup>a</sup>, D. Fouchez<sup>e</sup>, D. Hardin<sup>b</sup>,  
V. Le Brun<sup>h</sup>, J.M. Levy<sup>b</sup>, A. Mazure<sup>h</sup>, R. Pain<sup>b</sup>, R. Pello<sup>f</sup>,  
J. Rich<sup>g</sup>, R. Sadat<sup>f</sup>, K. Schahmaneche<sup>b</sup>, A. Tilquin<sup>e</sup>

<sup>a</sup>*IPNL, Lyon, France*

<sup>b</sup>*LPNHE, Paris, France*

<sup>c</sup>*CRAL, Lyon, France*

<sup>d</sup>*IAS, Orsay, France*

<sup>e</sup>*CPPM, Marseille, France*

<sup>f</sup>*OMP, Toulouse, France*

<sup>g</sup>*CEA/DAPNIA, Saclay, France*

<sup>h</sup>*LAM, Marseille, France*

---

## Abstract

For the years to come, the CFHT will be the best telescope to find large numbers of supernovae at high redshift thanks to its wide field imager, Megaprime. This data will permit to address very exciting scientific problems such as the cosmic star formation rate and the cosmological density parameters including a first measurement of the cosmic equation of state. To take full advantage of this unique capability, a coherent and ambitious program has to be setup and we support the basic scheme proposed by the Megacam Survey Working Group. We have studied some of the issues related to this survey: expected number of supernovae, exposure time budget, spectroscopy requirements, possible scenario and achievable precision on cosmological parameters.

---

## 1 Introduction

The measurement of the equation of state of Dark Energy has been proposed by the Megacam Survey Working Group (MSWG) as one of the scientific questions to be addressed by a large imaging survey of Type Ia supernovae (SN Ia) with Megaprime at CFHT [1]. Preliminary calculations indicate that constructing a Hubble diagram of SN Ia populated by about 700 objects up to redshifts of about 1 is within the reach of the instrument. We address here the possible scientific achievements of such a survey.

We first review the use of SN Ia supernovae for measuring the cosmological parameters and how it constraints the observations. We also briefly mention the interest of measuring the supernova rates as an important constrain on the cosmic star formation rate history.

In the following sections, we discuss the imaging survey, and in particular the achievable accuracies on SN Ia peak brightnesses when used as distance indicators. We then argue for the need of complementary spectroscopic observations and give a realistic estimate for an observation time budget on 8-m class telescopes. Finally, expected accuracies on cosmological parameters are computed in a specific scenario.

In section 11, we briefly show how the collected data may shed light on other science goals, including the closely related study of evolution of SN Ia and in section 12 we shortly address the data reduction requirements. In an appendix, we provide the key plots and tables obtained for an other observing scheme proposed by R. Carlberg.

This study does not intend to give a final answer on how to carry out the proposed survey. Figures provided here are primarily for comparison and checks and should be viewed as tools and inputs to help maximize the scientific outcome of the supernova part of the CFHLS.

## 2 Building the Hubble diagram of Type Ia supernovae

The Hubble diagram of SN Ia Supernovae plots their peak brightness as a function of redshift. This peak brightness is estimated from a fit of a template to light curves taken within a few weeks (rest frame) from the maximum light.

The scatter of intrinsic luminosity of SN Ia is dramatically reduced when one corrects the measured peak brightness for the now well known correlation between intrinsic luminosity and rate of decline. The photometric measurements

should then aim at measuring both peak brightness and rate of decline<sup>1</sup>, which was the observable quantity historically found to correlate with intrinsic luminosity. There are however very good indications that the rising part of the light curve is affected in the same way, i.e. that the rate of decline and rate of rise both correlate with the intrinsic luminosity. Perlmutter *et al.* [14] have adopted a single parameter to describe both : the “stretch” parameter. It modifies the light curve template as an expansion factor on the time axis (on top of its expected time dilation from redshift), w.r.t an average SN Ia. This makes use of all points along the light curve.

More classically, one should also correct for host galaxy extinction, measured through a color indicator, usually rest frame  $B - V$ . This requires the measurement of two filters corresponding roughly to rest frame  $B$  and  $V$ . For redshifts beyond  $z \sim 0.9$ , rest frame  $V$  goes beyond reach of silicon detectors, and would require observation with IR devices. Furthermore, the increasing sky brightness makes the measurement rapidly unaffordable, especially if one aims at measuring more than a few objects. The question of using rest frame  $U - B$  as an extinction indicator is of major interest when trying to push the highest redshifts accessible from ground. One key concern here is the “standardity” of SN Ia in  $U$ -band, a question still to be settled. The Nearby Supernova Factory [2], to be started around the same dates as Megaprime, should provide this crucial information.

It is fortunate that supernovae have their highest flux in the  $B$ -band, which can be measured up to redshifts of  $z = 1$  with silicon devices. To avoid the shortcomings of large  $k$ -corrections, one should however measure fluxes of objects at different redshifts in roughly the same rest frame band. This implies that observations are to be made in 4 bands ( $g'$ ,  $r'$ ,  $i'$  and  $z'$ ), in order to cover redshifts range from  $z \sim 0.3$  to  $z \sim 1$  needed to measure the cosmological parameters.

Finally, the Hubble diagram of SN Ia should contain as little as possible contamination from other transient objects, and relies on precise enough redshifts measurements. This implies that complementary spectroscopic observations have to be set up for both supernova identification and host galaxy redshift determination.

---

<sup>1</sup> The rate of decline is in practice described as the brightness drop in 15 rest frame days, called  $\delta m_{15}$ .

### 3 Measuring supernova rates

Measurement of the SN Ia rate allows one to probe the past history of star formation, since there is a time delay between the formation of stars and the occurrence of the explosion. Type II SN rate are also of interest to constrain the cosmic star formation rate (CSFR) since they directly probes the instantaneous star formation rate because of the short-lived massive stars which explode.

The large number of SN Ia that will be detected up to redshift 1 will give a measurement of CSFR up to redshifts  $z \sim 1.5$  probing a particularly interesting redshift range. The large statistics will further make it possible to measure the rates per host galaxy type.

The survey will also make it possible to detect large number of other supernova types such as Type Ib/c (SN Ib/c) and Type II (SN II). Current observations show that about 1 SN II or SN Ib/c is detected for 10 SN Ia. This is mostly due to the fact that SN II, although about 5 times more numerous are often much less luminous than SN Ia and therefore out of reach in magnitude limited searches. Current searches have not been optimized for SN II detection which is more difficult since SN II are most of the time much less bright than their host galaxy. Detecting SN II requires very efficient image subtraction techniques where a few percent increase of the luminosity of a galaxy has to be detected. Nevertheless, systematic residuals on image subtraction smaller than 1 % on the core of bright objects have been obtained on deep images observed with the CFH12k. This gives more flexibility to adjust the supernova detection cuts and the possibility to get a larger fraction of SN II detection on demand.

The survey strategy will permit to gather an unprecedented number of supernovae of all types and other transient objects provided identification of these events is done. This in principle means obtaining spectroscopic identification of every one of these objects all along the survey. However, the excellent quality of multiband photometry that the survey will provide for most of these events should allow developing, in the course of the survey, alternative strategies based on photometry, therefore reducing *in fine* the need for extensive spectroscopy.

## 4 The continuous sampling mode

### 4.1 Observing mode

As proposed by the MSWG, the survey should work in a continuous sampling mode rather than in a “triggered” mode as done so far in the SN Ia surveys. The (now classical) “triggered” mode consists namely in three steps and kind of observations:

- (1) **Search:** an area of the sky is observed at 2 epochs about 3 weeks apart, and light increases are detected via image subtraction. Typical cuts are a signal to noise ratio (S/N) greater than about 6 on the image subtraction and a light increase of at least 10 %.
- (2) **Spectroscopic confirmation:** the candidates are observed with a spectrograph for spectral identification and the redshift are measured with spectroscopy of the host galaxies.
- (3) **Photometric follow-up:** the spectroscopically confirmed candidates are observed for 6 to 8 weeks, in order to measure their light curve. For most of the objects, the follow-up does not cover earlier than a few rest frame days before maximum light. It is only by chance that a few objects of the available SN Ia catalog were sampled in the rise of the light curve.

Megaprime, thanks to its wide field, makes it possible to merge steps 1 and 3 into the same observations. Spectral identification (step 2) still has to be triggered, however with a series of photometric points rather than a single difference. This mode of operation has obvious advantages:

- The photometric sampling is of the same density before and after maximum light. This improves both the maximum light and light curve stretch estimations. It may also prove to be a good handle on possible evolution of SN Ia.
- The detection scheme used in the triggered mode biases the sample of objects in an unknown way. With a continuous sampling, more information is available to trigger spectroscopic identification in an unbiased way.

Since the program takes advantage on the multiplexing that the large Megacam fields enables, the same field should be observed as long as possible to reduce the number of objects for which either end of the light curve is missing. Using SN Ia for cosmology demands a precise measurement of the magnitude at maximum and of the stretch which means long enough sampling of the light curve with good signal to noise measurements on individual points. In practice, this means observing each SN light curve from at least 10 days before maximum to 15 days after maximum. Assuming 6 dark runs in a row as the maximum monitoring time for a given field, the time interval which allows a

measurement of the light curve for 25 days rest frame ([-10 days,+15 days]) is then  $T(z) = 158 - (1 + z) * 25$  days, taking into account the fact that observations will start 9 days before the first new moon and end 9 nights after the last new moon, which are separated by 140 days.

#### 4.2 Expected number of supernovae

The measured rate of SN Ia supernovae indicates a total explosion rate of about 150 SN Ia supernovae per square degrees and per year, up to  $z=1.2$  [3]. This figure is based on measurements done at  $z = [0.4-0.8]$  and assumes an explosion rate independent of redshift up to  $z = 1.2$ . About 30% of the SN Ia will be at  $z=[0.4-0.8]$  and  $\sim 50\%$  will be above  $z=0.8$ . Large numbers of SN Ib/c and SN II will also be detected.

In Table 1 we give an estimate of the expected number of SN Ia and SN Ib/c+II that will be observed during the 5 six months periods of the survey as proposed by the MSWG (4 square degrees). These numbers have been derived requesting that the [-10,+15] rest frame days part of the light curve is observed. The

Redshift	0.3	0.4	0.5	0.6	0.7	0.8	0.9	1.0	1.1	1.2	total
Ia	44	64	82	97	109	117	122	125	126	126	1014
Ib/c+II	110	150	180	150	110	-	-	-	-	-	700

Table 1

*Expected number of SN Ia and SN Ib/c+II in the survey proposed by the MSWG, requesting that [-10,+15] restframe days from maximum light are observed, and for 4 fields, 5 years, and 6 new moons monitoring of each field. About 1400 SN Ia have their maximum light during the observations.*

expected number of SN Ib/c+II has been computed assuming a flat luminosity function between -15.5 and -17.5 for these events and a total explosion rate 5 times higher than the SN Ia rate. It was further assumed that SN II+Ib/c can be efficiently detected by image subtraction.

## 5 Photometric performances

A realistic simulation including the instrument sensitivity, the sky brightness, airmass, moon, weather, extinction and seeing was developed to estimate the performances of Megaprime. Results of the simulation have been compared to the measured performances of the CFH12k and then used to built supernova light curves.

## 5.1 Megaprime simulation

### 5.1.1 Instrument sensitivity

The electron counting rate expected from a source of known spectrum has been computed for the Megaprime setup. To do that the spectrum is propagated through the optical components (mirror, corrector, filters, CCD), and finally integrated over wavelength.

The transmission of Megaprime filters was described according to [5]. The transmission curves used in the simulation can be found on [6]. [Note the strange feature of this data where the i' and z' filters are disjoint, at variance with the SDSS set as displayed on [7].] We obtained the following zero points:

	g'	r'	i'	z'
simulation	27.31	26.61	26.06	24.40

Table 2

*Zero points computed for Megaprime. These zero points are the (Vega) magnitudes of an object that yields 1 electron/s at zero airmass (assuming a Vega-like spectrum). We did not derive a value for u', which lacks QE data on the blue side of the band.*

To check the procedure, we computed the zero points of the current CFH12k camera assuming the same corrector transmission as for Megaprime, and for epitaxial CCD's as CCD9. These estimations can be compared to the mea-

	B	V	R	I
measurements [4]	26.37	26.57	26.52	26.22
simulation	26.51	26.56	26.46	26.35

Table 3

*Zero points computed and measured of the CFH12k camera (CCD9, epi flavour). These zero points are the (Vega) magnitudes of an object that yields 1 el/s at zero airmass (assuming a Vega-like spectrum for the values from simulation).*

surements from [4]. The agreement is at the 10% level, which is fair given the uncertainties of the ingredients of the simulation. A preliminary Z' zero point of 25.54 for CCD4 was recently determined by E. Magnier. It agrees at the same level with our simulation.

### 5.1.2 Sky brightness

To compute the expected sky brightnesses, we made use of a Mauna-Kea sky spectrum [10] and propagated it through the whole instrument.

We again checked that our predictions are consistent with the measurements available for the CFH12k. The comparison was performed in electrons/sec/pixel rather than in magnitudes per unit solid angle, because of the large sky color terms. The simulation gives a flux higher than the measured one by a factor of 1.5 to 2 at the red end. This disagreement is currently not understood. To reproduce the measured electron counts, we applied a linear correction to the sky spectrum. The predicted sky brightness as well as the measurements are given in Table 4. To account for the increase of sky brightness due to air-

	B	V	R	I	Z
measurements (CCD9) [4]	1.5	4.5	7.8	18.0	-
simulation (epi)	1.7	4.8	6.7	19.0	13.0
measurements (CCD4) [8]	-	-	6.5	25	22.5
simulation (high $\rho$ )	1.3	4.6	7.3	25.0	23.4

Table 4

*Sky brightness (in electrons/sec/pixel) measured and simulated for the CFH12k. The measurements apply to a dark sky at airmass = 1.*

mass and moon, we applied the measured dependencies given in Table 5 as multiplicative factors [4,8].

	B	V	R	I	Z
airmass = 1.5	1.15	1.3	1.3	1.38	1.70
moon = 0.5	3	2	1.3	1.1	1.05

Table 5

*Sky brightness correction factors for airmass and moon*

### 5.1.3 Limiting magnitudes

Using the instrument sensitivity and sky brightness derived above, we computed the limiting magnitudes, defined following DIET [9] prescription for point sources: the flux is integrated in an aperture of diameter  $1.45 \cdot \text{FWHM}$ , which contains 64 % of the total flux<sup>2</sup>. Better than 0.1 mag agreement was achieved when comparing with DIET tables in the case of the CFH12k instrument.

For Megaprime, we therefore predict the limiting magnitudes of table 6.

<sup>2</sup> The quoted magnitudes refer of course to the total flux, since they should not depend on the chosen photometry technique.

	g'	r'	i'	z'
limiting mags	26.35	25.50	24.85	23.40

Table 6

*Limiting (Vega) magnitudes computed for Megaprime. We considered point sources observed at a seeing of 0.8", airmass=1, with a dark sky, detected at the 5  $\sigma$  level in 1800 s. See [9] and this text for the assumptions on the photometry technique.*

#### 5.1.4 Observing conditions

Light curve reconstruction is particularly sensitive to varying observing conditions. We accounted for time lost to weather, extinction and seeing distribution, using a simulator from J. Tonry based on real CFH12k observations. We used a sample provided by R. Carlberg and obtained the following averages (see Figure 1):

- 25% of a night is lost to weather.
- the extinction is less than 0.1 mag (we do not know in which band, but we assumed that this figure was pessimistic for the reddest bands).
- the seeing averages to 0.85" (median is 0.81").

This simulator provides correct correlations between the 3 variables.

## 5.2 Simulation of Type Ia supernovae light curves

To compute the expected flux from SN Ia, we rely on a time sequence of spectral templates, based on high S/N spectroscopic observations of nearby objects, and complemented by interpolations and simulations where data was missing [11].

The time sampling is of one rest frame day, from 14 days before maximum light (in  $B$ -band) to 46 days after. We normalized the SN phases relative to each other using the empirical light curve template from [12], and also extended the time range toward the explosion date by scaling the earliest spectrum (-14 days) to the observed light curve.

We used an intrinsic brightness of  $M_B = -19.46 + 5 \log H_0/63.3$  [13] as our overall brightness normalization.

Figure 2 gives the peak magnitudes for SN Ia as a function of redshift. Although the procedure allows to predict the flux in any rest frame band where template spectra are available, one should only trust the predictions for the bands close enough to rest frame  $B$ -band.

The Monte-Carlo simulation was done typically using a few thousands light

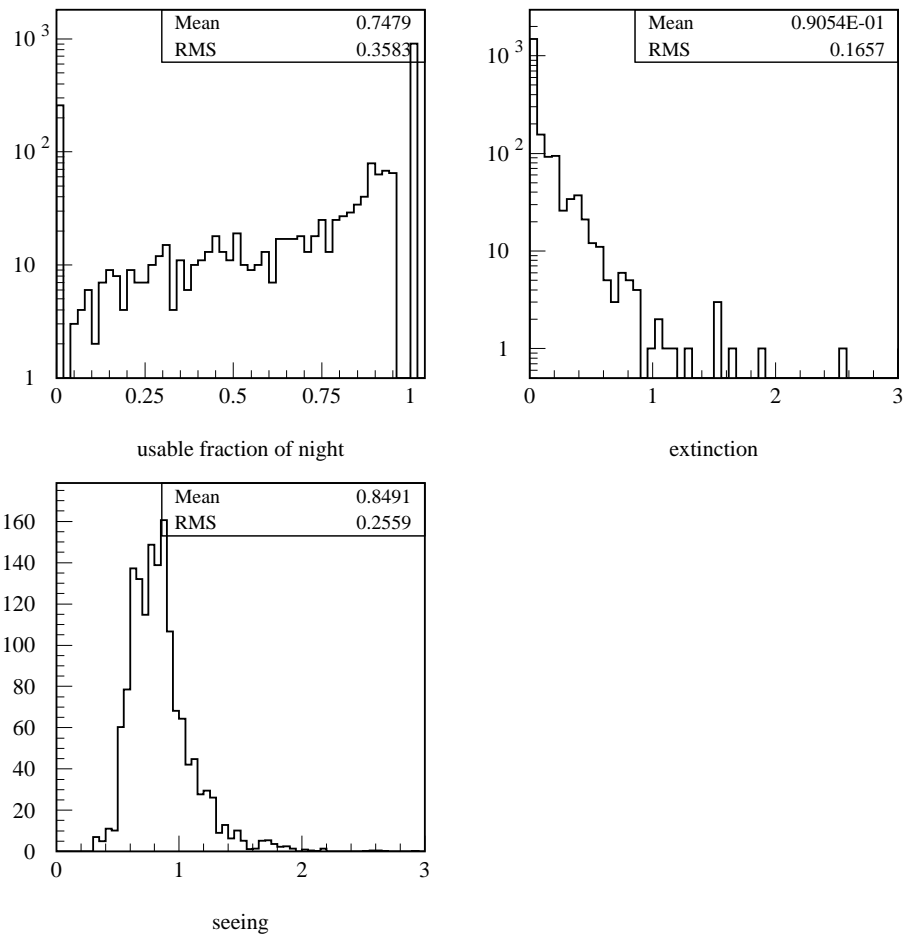


Fig. 1. *Weather statistics used in the simulation.*

curves, sampled in one photometric band and fitted. The following procedure was applied :

- choose a redshift either according to a distribution (which follows the volume), or as a fixed value.
- generate a light curve for this redshift and observing band. For each observing date on the light curve we:
  - randomly perform an observation according to the fraction of the night available to observations (given by the “weather simulator”).
  - compute the sky background spectrum according to the moon phase, and the airmass (all observations were simulated at airmass=1.3).
  - compute the atmospheric extinction for the airmass, and an additional extinction given by the “weather simulator”.
  - propagate the supernova spectrum at this phase through all optical components including atmosphere and filter, and integrate over wavelength

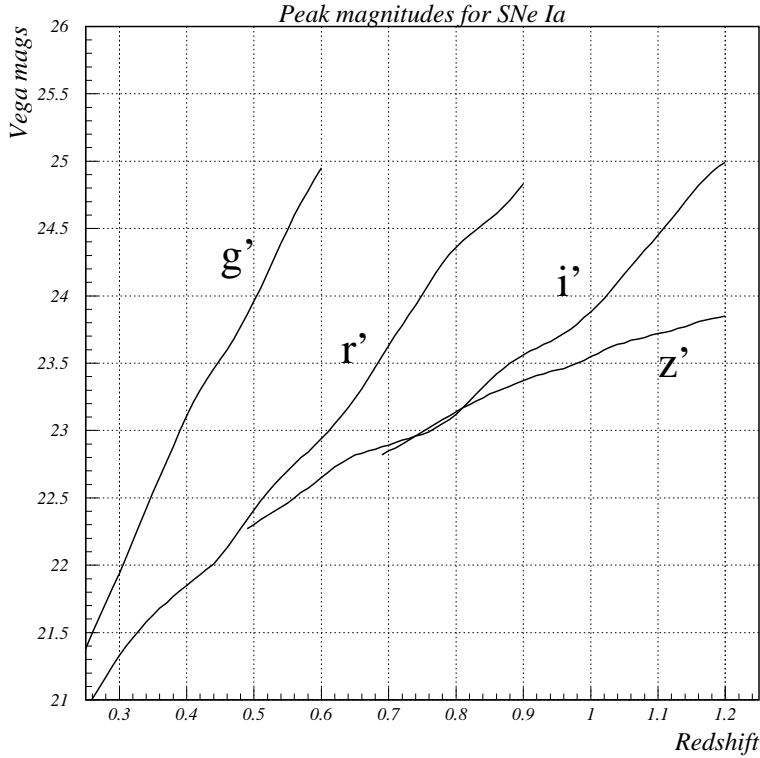


Fig. 2. Average SN Ia peak magnitudes (Vega) as a function of redshift for a cosmology  $(\Omega_M, \Omega_\Lambda) = (0.28, 0.72)$ , assuming no host galaxy extinction.

to get the number of electrons. We then lower it by photometry aperture losses (.64 by default).

- propagate the sky spectrum through all optical components and count the number of electrons in the photometry aperture, defined using the seeing given by the “weather simulator”.
- randomize the expected supernova signal (which may be 0) according to the sky background fluctuations.
- perform a 3 parameters  $\chi^2$  fit of the observations with:

$$\chi^2 = \sum_i \frac{(f_i^{\text{measured}} - \mathbf{f}_{\text{max}} T((t_i - \mathbf{t}_{\text{max}})/\mathbf{s}))^2}{\sigma_i^2}$$

where the sum runs over observations,  $\mathbf{f}_i^{\text{measured}}$  is the measured flux,  $T$  is the flux template (for this redshift and band),  $\mathbf{t}_{\text{max}}$  is the date of maximum, and  $\mathbf{s}$  is the stretch. The template is defined so that the average stretch is 1.

Resolution on light curve parameters can then be derived by comparing generated and reconstructed quantities. Note that the simulation does not account for supernovae host galaxy light, which adds a small amount of noise. We also

neglected the fact that subtracting the host galaxy involves additional noise present on the final reference image(s) without the supernova, since the proposed observing scheme makes it possible to build a very deep final reference image.

### 5.3 Simulations of $i'$ light curves at $z=0.8$

In order to assess the impact of photometric sampling and weather, supernovae light curves were simulated in various observing conditions. All these virtual experiments were done at redshift  $z = 0.8$ , in the  $i'$ -band and with an exposure time of 1800s per observation. Observations were assumed to start 9 nights before new moon and end 9 night after new moon, and to be carried out at all lunations. Only measurements prior to 35 rest frame days after maximum light were considered, because of the stretch behavior which may not hold beyond this date.

Events for which the observing schedule did not allow to sample the interval  $[-10,+15]$  rest frame days from maximum, and which had less than 8 measured points were rejected. The results are summarized in Table 7.

simulation conditions	$\sigma(m_{peak})$	$\sigma(s)$	$\sigma(m_{peak})[corrected]$	N/S
seeing=0.8, frac = 1 extinction=0, 7 obs/lunation	2.36	2.56	4.44	4.86
same as above, frac = 0.75	2.99	3.31	5.49	4.86
use “weather simulator”	2.78	3.13	5.20	5.37
same as above, 9 obs/lunation	2.65	2.92	4.93	5.37

Table 7

*Photometric resolution (in %) obtained under various sampling hypotheses. The peak brightness of our samples is  $i'=23.15$ (Vega). The last column gives the noise to signal (N/S) of a single measurement at peak. “frac” denotes the fraction of nights where observations can occur. The third row represents a favorable realization of the weather (83% of the time could be used).*

From the results summarized in Table 7, we conclude that:

- The random loss of photometric samples applied from row 1 to 2, affects the resolution more than expected just from the loss of observing time. This is due to the fact that some of samples lost result in an increase of the full moon gap. This stresses the need for setting a very high priority for the observations of supernovae at the beginning and the end of the lunation.
- The resolution gain when going from 7 to 9 points per lunation (third to fourth row) is less than  $\sqrt{9/7}$  (in which case the resolution for the fourth

row would be 4.58%). This again points out that the full moon gap should be kept as short as possible.

## 6 Imaging survey strategy

A priori the measurement of the cosmological parameters requires extending the redshift range as much as possible. This is based on the fact that cosmological effects are more important at higher redshifts. This however should be weighted by the “cost” of detecting, identifying and measuring a high redshift supernova compared to the sensitivity of the various cosmological parameters as a function of redshift. Optimization of the solid angle versus redshift range should therefore be performed to obtain the best possible measurement. This work remains to be done. In what follows we have assumed a solid angle of 4 square degrees as proposed by the MSWG.

### 6.1 Redshift range

The observable redshift range will be fixed by the available filters and CCD efficiencies. As shown in Figure 3, rest frame  $B$ -band can be measured up to redshifts of about 0.9 to 1, through a mixture of  $i'$  and  $z'$ . On the lower end of the redshift range,  $g'$  allows to measure rest frame  $B$ -band down to  $z \simeq 0.2$ , and up to  $z \simeq 0.4$ . In this redshift range, the photometry can be carried out accurately enough for systematic checks of the reductions to be done.

### 6.2 Peak Brightness resolution

Using the ingredients described in the previous section, we simulated supernovae in the redshift range from 0.25 to 1.25. We used the “weather simulator”, assumed 7 (scheduled) observations per lunation (-9,-6,-3,0,3,6,9 days w.r.t new moon). The resolution of the fitted peak brightness was evaluated using the dispersion of reconstructed quantities. Figure 4 gives the resolutions as a function of redshifts in the 4 different bands, assuming some plausible values for the exposure length.

### 6.3 Color measurement

Classically, host galaxy extinction is derived through the measurement of the color excess,  $E(B-V)$ . However, since cosmological measurements using SN Ia

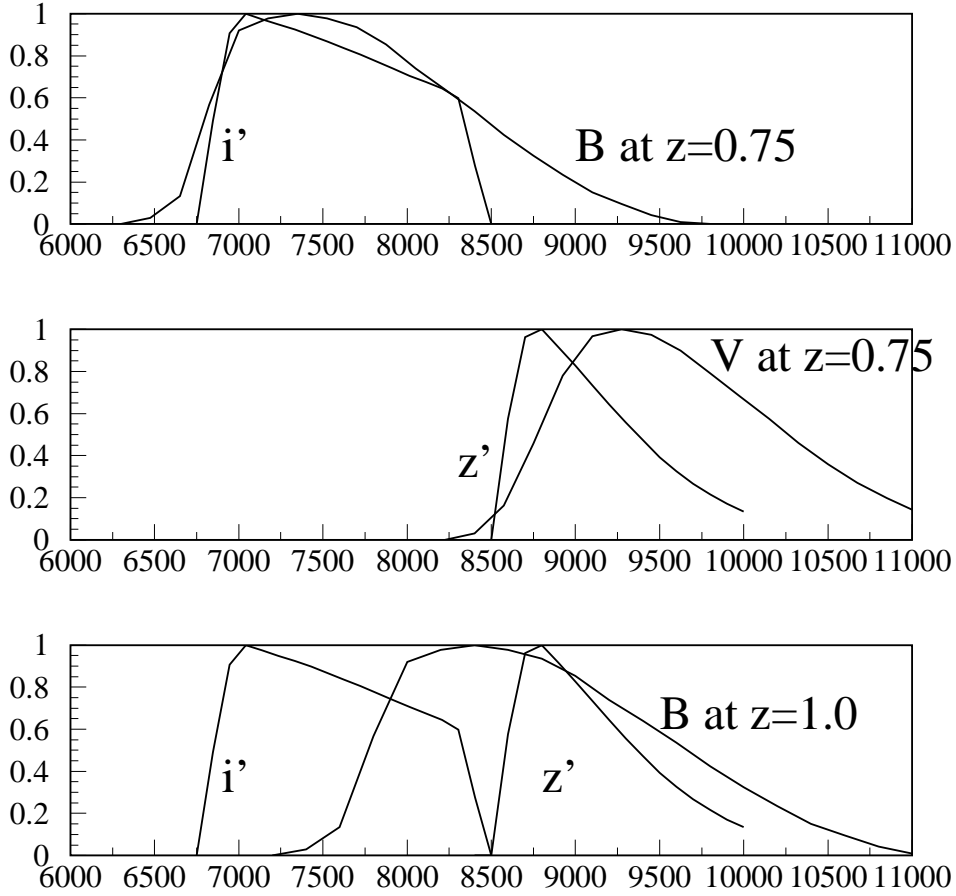


Fig. 3. Comparison of redshifted B-band and V-band Bessel filters with Megacam  $i'$  and  $z'$  filters, where the latter account for filters and all optical components.

rely on a comparison of nearby and distant objects, they are only sensitive to evolution of the average extinction rather than to the extinction itself. In their paper, Perlmutter *et al.* [14] did not actually correct for extinction arguing that average color of distant and nearby objects were identical within errors.

In the framework of supernovae light curves, the most precise color indicator is the fitted peak magnitudes difference, without stretch corrections. It makes use of all points on the light curves. As for the stretch, the color correction aims at providing a distance indicator as precise as possible.

First order stretch and color corrections can then be accounted for using:

$$B_{corr} = B_{measured} - \alpha(1 - s) - \beta(B - V).$$

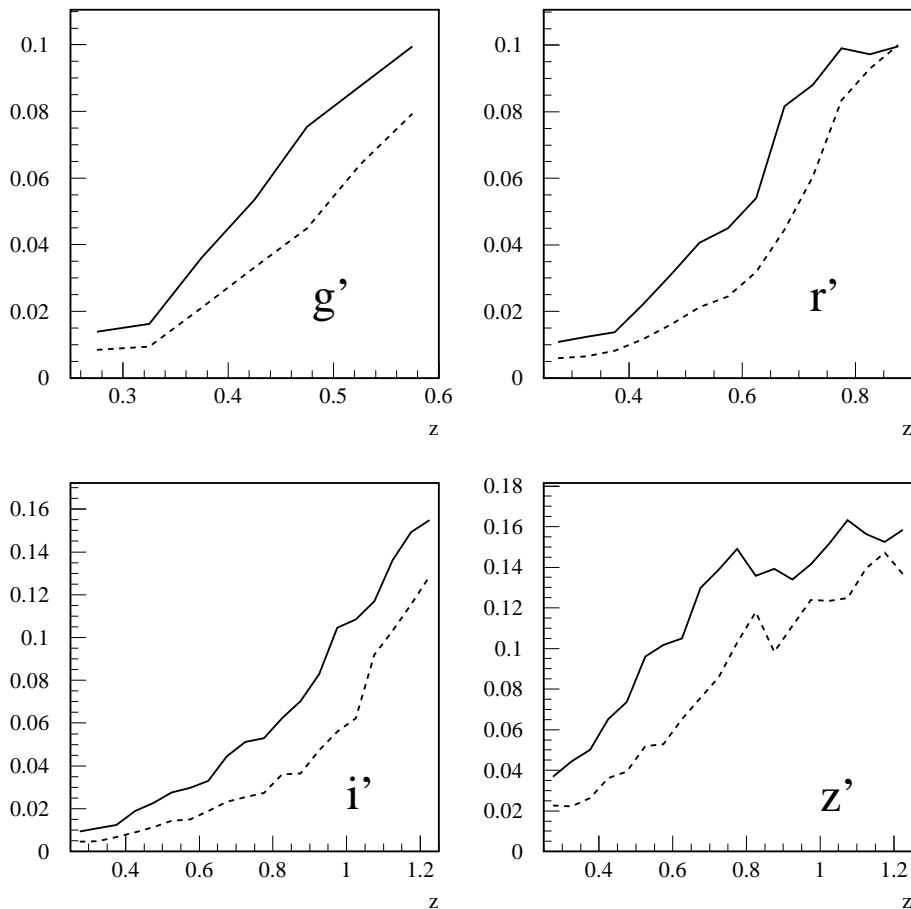


Fig. 4. *r.m.s* of fitted peak magnitude, corrected for stretch (full line) and uncorrected (dashed line). The assumed exposure times are 300 s in  $g'$ , 600 s in  $r'$ , 1800 s in  $i'$  and  $z'$ .

By minimizing the scatter of the corrected intrinsic peak brightnesses of nearby supernovae, N. Regnault [15] finds<sup>3</sup>  $\alpha \simeq 1$  and  $\beta \simeq 2$ , with errors of about 10 %. The color correction factor  $\beta$  is lower than the expected value (about 4), probably because without extinction, peak brightness and peak color correlate, in a way opposite to the effect of dust.

<sup>3</sup> The maximization was in fact done using the  $\delta M_{15}$  parameter rather than the stretch (although light curve were fitted using the stretch concept):

$$B_{corr} = B_{measured} - \alpha(\delta M_{15} - 1.1) - \beta(B - V)$$

$\alpha$  was found to be around 0.6. Since  $\delta M_{15} - 1.1 = 1.6 * (1 - s) + o((1 - s)^2)$ , our  $\alpha$  is approximately 1.

#### 6.4 Statistics and precisions over the redshift range

Using the data shown in figure 4, we can derive the precision of “corrected peak brightness” measurements (to be understood as distance measurements) as a function of redshift. The results are summarized in Table 8.

Redshift	1 year statistics	$\sigma_{peak}$	$\sigma_{int}$	$\sigma_{tot}$	$\sigma_{color}$	$\sigma_{color}\sqrt{N}$
0.3	9	0.015	0.15	0.15	0.01	-
0.4	13	0.02	0.15	0.15	0.015	-
0.5	16	0.035	0.15	0.15	0.025	-
0.6	20	0.045	0.15	0.156	0.03	-
0.7	22	0.05	0.15	0.158	0.08	0.015
0.8	24	0.055	0.15	0.16	0.10	0.02
0.9	25	0.07	0.15	0.165	0.10	0.02

Table 8

*Resolutions of stretch corrected peak brightness and color as a function of redshift. The statistics is for 4 fields (1 sq degree each) observed one semester 6 dark runs in a row.  $\sigma_{peak}$  is the resolution of the stretch corrected peak magnitude.  $\sigma_{int}$  is the intrinsic scatter of SN Ia (after stretch correction).  $\sigma_{tot}$  sums the two previous ones.  $\sigma_{color}$  is the precision of the color measurement. The last column gives the precision on the average color of a 0.1 redshift bin. Up to  $z=0.6$ , the color can be accurately measured on an event per event basis. The total statistics (for 1 year/4 fields) is 127 objects.*

#### 6.5 Total integration time budget

As an example of a possible survey strategy, we detailed in table 9 the integration time needed to perform the survey assuming that 4 square degrees will be observed in the four bands every third night during five 6 months period.

Note that these estimates include bad weather fraction, at variance with usual requests to QSO. One should nevertheless implement a scheme where observations lost to weather are done as soon as possible. This would improve the efficiency of the telescope time involved in this program (very sensitive to the size of the moon gap). Ray Carlberg proposes an algorithm to achieve this goal.

band	time per exposure (s)	1 semester (h)	5 years (h)
g'	300	3.5	17.5
r'	600	7	35
i'	1800	21	105
z'	1800	21	105
total (1 field)	4500	52.5	262.5
total (4 fields)	-	210	1050

Table 9

*Integration time in the different colors, assuming 7 observations per lunation, each field being observed 6 lunations in a row.*

## 7 Determination of the redshift

Building the Hubble diagram requires knowing the redshift of the supernovae. This is usually done by spectroscopy of the host galaxy. Past experience has shown that a simultaneous measurement of the SN and its host galaxy could often be achieved with a judicious alignment of the slit. This however is not always possible and additional spectroscopy time will be needed to get a spectrum of the host galaxy. An alternative method would be to use an integral field spectrometer (such as VIMOS on the VLT) to get both the SN and the host galaxy spectra simultaneously. This would further have the advantage of relaxing the need for precise positioning of the slit.

Note however that the spectrum of the galaxy does not have to be taken close to supernova discovery but can always be obtained long after the supernova has faded. For some cases even, where the host galaxy light contamination is large, it will be necessary to get a host galaxy spectrum after the supernova has faded to subtract the galaxy light from the supernova spectrum. This means that observing time on 8-m class telescopes will have to be allocated to measure the redshifts.

### 7.1 Photometric redshifts

A good estimate of the redshift can be obtained from multicolor optical photometry of the host galaxy. Determination of these photometric redshifts is based on template fitting of the galaxy and can reach precisions of  $\delta z \sim 0.05$  up to redshifts of  $z \sim 1$  [16]. Although a factor  $\sim 10$  better is needed to precisely extract the cosmological parameters from the Hubble diagram, the availability of photometric redshifts of all galaxies is essential. This information will be used to make a pre-selection of candidates according to their redshifts. This

is important for spectroscopy where rejection of  $z > 0.9$  candidates will have to be done to reduce the overall amount of spectroscopy time needed for this project.

Obtaining accurate photometric redshifts requires precise i.e. deep enough multicolor photometry of the fields. However this should not result in an increase of the time needed for the survey since repeated multicolor observations of the same regions of space will be done that will rapidly generate deep enough images. However adequate software and processing pipeline should be prepared well in advance to rapidly extract the information.

## 7.2 Spectroscopic redshifts

Measurement of the redshifts will have to be derived from spectra of the host galaxies. These spectra can be obtained either as additional observations on 8-m class telescopes or, when available, from existing spectroscopic survey provided the same regions of space are observed (see below choice of fields).

Spectroscopic redshifts are based on detecting either the 4000 Å break or absorption or emission lines such as O II  $\lambda 3727$ , O III  $\lambda 5007$  or H $\beta$  in the galaxy spectra. A crude estimation shows that the exposure time is not very redshift dependent and that, in most cases, 30 mn exposure should be enough to reach  $z \sim 0.9$  on 8-m class telescopes. With about 150 SN candidates per semester up to redshifts  $z = 0.9$ , this adds up to about 50 h per semester. Note again that these observations can be done long after the supernova has faded and that a fair fraction of this time could be saved if the observations can be coordinated with the deep spectroscopic surveys. This number should therefore be considered as an upper limit and could even get close to 0 with a judicious choice of fields.

Finally since the phase of the supernova candidates will be very well known from the light curve, an estimate of its redshift can also be derived from the SN spectrum itself, however with large uncertainties.

## 8 Identification of the supernova

Identification of the supernovae type is needed both for the measurement of cosmological parameters which relies on selecting SN Ia and to identify other SN types such as Ib/c and II in order to measure their respective rates to address the star formation rate history. It would also be of interest to get unbiased measures of the rates of all the other variable objects that will be

detected.

The supernova classification scheme is based on the identification of specific spectral features at or near maximum light. SN Ia, in particular should show prominent silicon absorption line at  $\lambda = 615$  nm in their spectra. However, observation of this feature is not always possible and SN identification sometimes relies on the observation of other spectral lines. Non spectral features for identification such as their light curves shape and brightness or the type of their host galaxy have also been suggested. These indirect identifications are subject to debate and remain in any case to be “calibrated” against the universally accepted spectral definitions. In particular, efficiencies and contaminations from other types will have to be measured before any identification scheme based on non spectral features is adopted. The high statistics that Megaprime will provide will allow one to do these measurements which could result in a dramatic reduction of the amount of 8-m spectroscopy time needed to identify the supernovae.

### *8.1 Trigger and pre-selection*

The continuous sampling strategy adopted for this survey makes it possible to monitor the rise of the supernova and trigger spectroscopy close to maximum light. The precise algorithm has to be defined but the magnitude and date of maximum light can in principle be estimated in advance using a simple extrapolation of the first three measured points of the light curve.

Obtaining one spectrum for every SN candidate, requires securing a fair amount of spectroscopy time on 8-m class telescopes which may be difficult to achieve. As discussed above, the quality of the data gathered in the survey together with additional information such as the photometric redshifts and the host galaxy type will be used to develop alternative classification schemes or simply selection algorithms during the first years of the survey. For example, SN Ia could be selected based on:

- their host galaxy type : although the statistics are currently very small, only SN Ia have been seen in E/SO. The morphology of the galaxies will have to be known in advance.
- their brightness : SN Ia are usually brighter than other SN types by  $\sim 2$  magnitudes. A preselection based on a cut on the estimated magnitude at peak at a given redshift could therefore be implemented. An estimate of the redshift of the galaxy will have to be known in advance.

The exact method and the final contamination after pre-selection is currently impossible to estimate due to the small statistics available. For that reason, it is important that before implementing any pre-selection scheme, a unbiased

sample of a few hundred supernovae is taken with spectral identification for everyone of them.

## 8.2 Spectroscopy time budget

Current experience shows that SN Ia spectra at redshifts up to  $z = 1.2$  can be obtained but the amount of spectroscopy time needed will vary a lot depending on whether we aim at simply identifying the supernova or making a detailed study of its spectrum for further studies.

Our goal for this survey is a simple identification of the supernova type. We have followed two different approaches to estimate the overall spectroscopy time budget needed to complete the experiment: a scaling of existing measurements done at Keck and VLT and a calculation based on a full simulation of observations.

Recent identification at Keck of a redshift 1.2 SN Ia close to maximum light was achieved with 130 mn exposure [19]. At this redshift, the Si II  $\lambda 4130$  line is used since the usual Si II  $\lambda 6355$  is out of reach. From this measurements and earlier ones done at Keck and VLT at redshifts ranging from 0.3 to 1.2 we estimate that about 60h integration time on a 8-m class telescope would be needed to identify the  $\sim 100$  supernovae (Ia, Ib/c, II) per square degree that will be discovered up to  $z=1.2$  each semester. Note that more than 2/3 of the time would be spent on  $z > 1.0$  candidates (3/4 of the time on  $z > 0.9$ ).

The second estimate is based on simulating the observation of SN Ia spectra with the FORS instrument on the VLT. The simulation takes into account the technical parameters of the telescope (seeing, airmass, response of the different apparatus, sky noise spectrum, ...) and returns the spectrum as recorded on the CCD. It is then possible to estimate the exposure time as a function of the redshift for a given signal to noise ratio (S/N). The identification is based on the same Si II  $\lambda 4130$  line as previously done since the Si II  $\lambda 6355$  is out of reach for  $z > 0.5$  supernovae. We define an average S/N between 350 and 470 nm to identified Ca H and the Si at 400 nm in the rest frame and found that a  $S/N > 5$  for a bin of 10 Å is required to properly identify a SN Ia. Under these conditions, an 8-m telescope such as the VLT can identify supernovae at a redshift of  $z = 0.9$  with an exposure time of 1 hour. This estimation is in agreement with the existing VLT measurements.

We conclude that a strategy aiming at selecting  $z < 0.9$  candidates should be pursued, using for example available photometric redshifts, to reduce the amount of spectroscopy time needed. In such a scheme about 80 h integration time by semester on a 8m class telescope would be needed to identify the  $\sim 400$  supernovae (Ia, Ib, II) at redshifts ranging from 0.3 to 0.9 that would

be discovered in 4 square degrees survey. This is a large number although not out of reach considering the fact that several 8m class telescopes are now available to our community. We finally point out that this time will have to be scheduled in a distributed way such as for example as 1 hour/night every third night during the semester to guaranty near maximum light spectroscopy of all candidates.

## 9 Choice of fields

A priori the fields can be chosen in any region of the sky provided the selected region is free from bright stars, not obscured by dust and visible for 6 months per year. To allow follow-up at VLT, at least a fraction of the fields should be around equator.

It would be very useful however to benefit from information such as galaxy morphology, photometric redshifts or even spectroscopic redshift of galaxies prior to the survey. Such information could be available at the start of the survey on selected area from large surveys such as VIRMOS [17] at the VLT or DEEP [18] at Keck. Coordination with these projects should therefore be studied. For fields for which this information will not be known prior to the survey, a complementary program aiming at determining their photometric redshifts should be set up either prior to the survey or at its very beginning since it will permit saving a lot of precious 8-m spectroscopic time.

If one targets the 4 VIRMOS fields, observing them 6 dark runs in a row imposes a Megacam run at every new moon. Relaxing to 5 dark runs (for one or 2 fields) makes it possible to allocate one new moon (around june/july) to other dark time instruments.

## 10 Precision of cosmological parameter determinations

We consider two different cosmological models: The “classical” model in which the cosmic state equation parameter,  $w$  is equal to -1, parametrized by  $(\Omega_M, \Omega_\Lambda)$  and a second model in which the universe is flat with a Dark Energy component of unknown equation of state, which we parametrize by  $(\Omega_M, w)$ .

Note that with the redshift distribution accessible at CFHT (i.e. typically from 0.3 to 0.9), and even if one adds a sizable sample of nearby objects, a cosmological fit to  $(\Omega_M, \Omega_X, w)$  is almost degenerate and does not provide useful measurements without external constraints.

In the fitting procedure, the intrinsic brightness  $\mathcal{M}$  of SN Ia has to be accounted for. For small samples, one usually uses determinations from well measured nearby objects. For higher statistics, this parameter has to be extracted from the data and marginalized over. This nuisance parameter has an large impact on the achievable precision [20] and the redshift distribution accessible in the survey requires adding a sample of nearby objects to fully constrain the cosmological parameters. Unless otherwise stated, the precisions we quote account for this parameter.

We considered a sample of 200 nearby objects at  $z = 0.03$  that we added to the CFHLS sample. Such a set of well measured objects could for example be available from the Nearby Supernova Factory. We checked that our results were not sensitive to the exact amount of nearby objects, which indicates, that even when we quote precisions that involve these objects, these precisions scale with the square root of the CFHLS statistics (within a factor of 2 of the 750 objects we considered). We also checked that the redshift of those nearby objects can be varied around 0.03 without a dramatic impact.

Finally, we want also to emphasize the fact that these results assume a precision on  $z$  better than 1 % (an 1% error on  $z$  gives a 10 % relative error on parameters). This explain why a spectroscopic  $z$  measurements with a precision better than 1 % are requested for all supernovae.

Using the precisions of Table 8 and assuming the 5 six months periods operation, we derived Fisher matrix precisions for the 2 cosmological models defined above. The results are reported in Table 10.

Model	samples	prior(s)	$\sigma$	$\rho_{XY}$
$(\Omega_M, \Omega_\Lambda)$	CFHLS	-	(0.12,0.37)	0.95
$(\Omega_M, \Omega_\Lambda)$	CFHLS+NEARBY	-	(0.06,0.10)	0.95
$(\Omega_M, w)_{\text{flat}}$	CFHLS	$\mathcal{M}$	(0.06,0.15)	-0.994
$(\Omega_M, w)_{\text{flat}}$	CFHLS + NEARBY	-	(0.07,0.18)	-0.98

Table 10

*Precisions obtained for the determination of cosmological parameters for various schemes and samples assuming a 5 years operation. “NEARBY” refers to a sample of 200 objects at  $z=0.03$ .*

Figure 5 shows the confidence contours for a measurement of  $(\Omega_M, w)$ , and a measurement of  $(\Omega_M, \Omega_\Lambda)$  after 5 years of operation (1 semester per year).

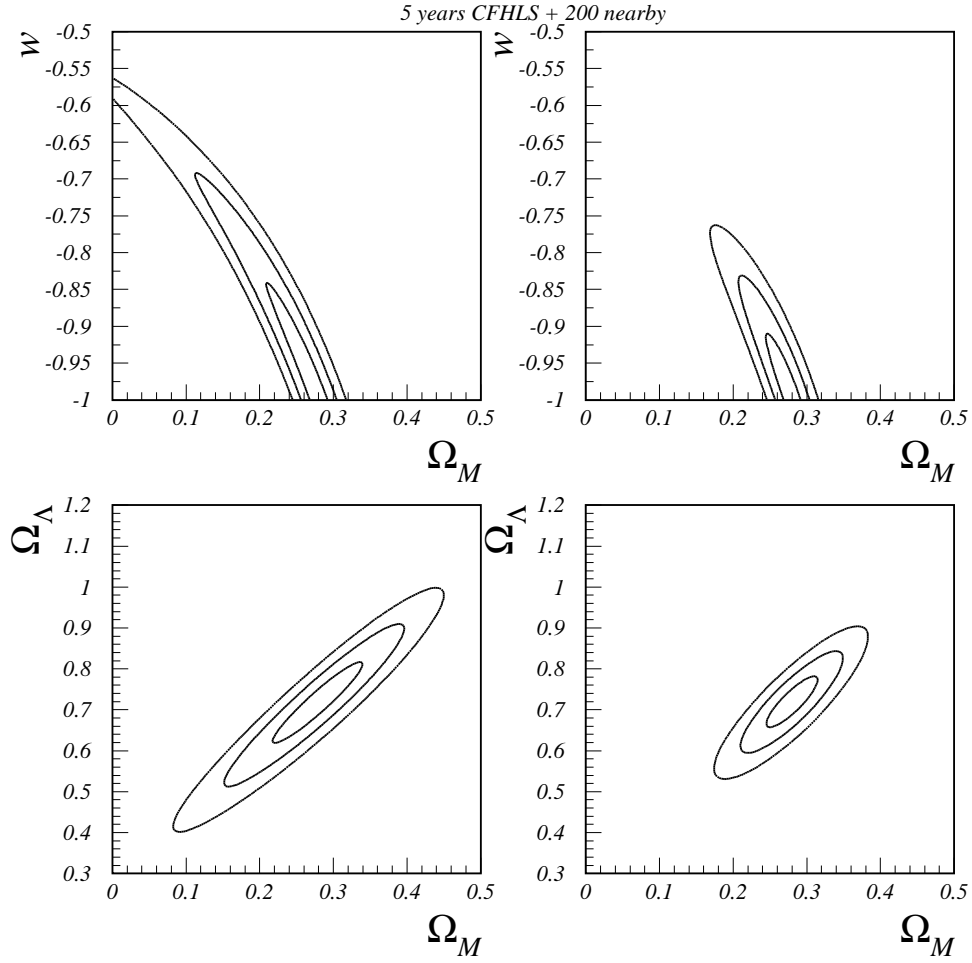


Fig. 5. One, two and three  $\sigma$  contours (39 ,86 and 99 % CL) for the  $(\Omega_M, w)$  (top) and  $(\Omega_M, \Omega_\Lambda)$  cases for the whole CFHLS statistics + 200 nearby objects. The assumed values for the cosmological parameters are  $\Omega_M = 0.28$ ,  $\Omega_\Lambda = 0.72$  and  $w = -1$ . The plots on the right add a gaussian prior of  $\Omega_M$  with  $\sigma=0.03$  (i.e  $\sim 10\%$ ). All these contours are obtained after marginalisation over SN Ia average intrinsic brightness.

## 11 Other scientific targets

### 11.1 Higher redshifts supernovae

The survey will detect a large number of supernovae at high  $z$  for which Megaprime will not be able to provide well enough measured color or even light curve. For these very distant supernovae ( $z > 0.9$ ) additional observation will be needed and could be set up in complementary programs.

## 11.2 Spectral study of distant SN Ia

The large number of supernovae that will be detected and followed-up will permit very valuable spectroscopic analyses of supernovae in the full redshift range and at all phases of the supernovae. This is of great importance for this project since it will allow quantitative study of SN evolution from precise spectral information. For that purpose additional spectroscopy time will be needed but could probably be requested on a complementary proposals basis.

## 12 Data processing

Rapid processing of the images will have to be performed in order to assess the quality of the data, find the candidates and decide within a few hours to get a spectrum.

The processing chain will include data reduction, image shifting and coaddition, reference image construction, subtraction to find supernovae candidates, follow up of previous candidates to construct light curves and trigger to request a spectrum close to maximum. This last step will probably require getting information on the host galaxy : morphology and/or photometric  $z$ .

The supernovae detection and follow-up chain should be hooked up to the CFHT online data processing chain. A possible sketch of the data flow for this processing is given in Figure 6. Online processing will require automating most of the analysis steps. Human intervention will probably stay necessary but should be minimized.

Prototype software has been developed for the processing of CFH12k images and is currently running on CFHT computers. The current software allow fast processing of images and quasi online detection of supernova candidates. This software will have to be robustified and automated to routinely process the Megacam data flow. Additional software will have to be implemented to perform light curve reconstruction and trigger decision needed for spectroscopy. We estimate that this work will require between 2 and 4 year $\times$ man to be completed. Additional hardware will also have to be acquired to cope with the increase data flow.

## CFHLS SNe online processing

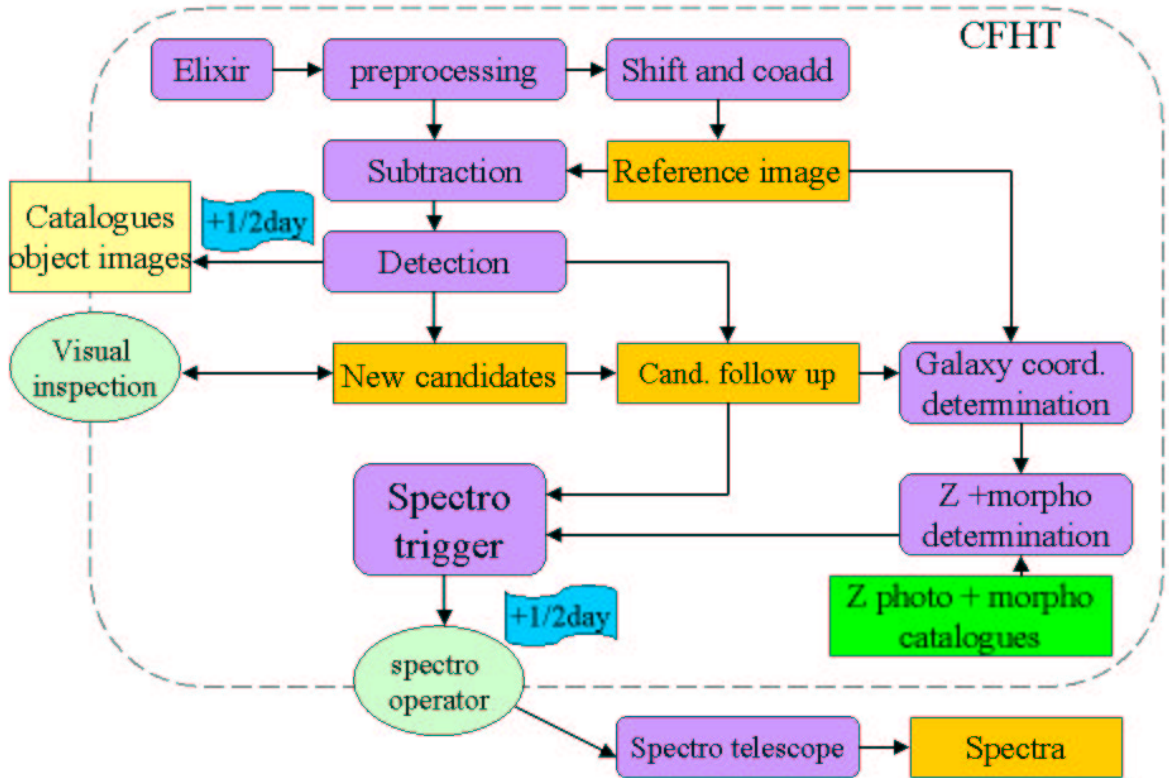


Fig. 6. *Supernova online processing data flow.*

## 13 Summary

We have computed the number of Type Ia supernovae expected in the proposed scheme of the CFHLS as well as an estimate of expected number of Type Ib/c and Type II supernovae. A detailed simulation of Megaprime has been developed to simulate supernovae light curves and compute the expected peak magnitude precisions over the accessible redshift range. We propose to set up a program in which spectral identification of the supernovae is done up to redshift  $z \sim 0.9$ . We estimated the amount of spectroscopy time needed on a 8 m class telescope and found that a reasonable figure emerges. In this scheme precise results can be obtained on the measurement of cosmological parameters and in particular on the equation of state of the dark energy. This strategy will further allow us to get very important results on the supernovae rates as a function of redshift for all supernovae and host galaxy types, a key ingredient for the understanding of the star formation rate.

## Acknowledgements

We benefitted a lot from discussions with Jean-Charles Cuillandre and E. Magnier about the CFH2k. Their new measurement of the sky level was triggered by our questions. We used a Mauna-Kea weather simulator developed by J.Tonry. The SN Ia light curves were generated from a set of template spectra assembled by P. Nugent.

## References

- [1] The CFHLS: report by the MSWG to the SAC. See :  
<http://www.cfht.hawaii.edu/Instruments/Imaging/Megacam/MSWG/#010228>
- [2] see <http://snfactory.in2p3.fr>
- [3] Pain, R. et al., *Apj* 1996. (update submitted *ApJ*)
- [4] CFH2k optics: See :  
<http://www.cfht.hawaii.edu/Instruments/Imaging/CFH12k/Summary/CFH12K-Optics.html>
- [5] Megacam filters. See :  
<http://www.cfht.hawaii.edu/Instruments/Imaging/Megacam/MSWG/Filters010504.html>
- [6] <http://supernovae.in2p3.fr/~astier/simdata/>
- [7] Megacam SDSS filters. See :  
<http://www.cfht.hawaii.edu/Instruments/Imaging/Megacam/MSWG/Filters010403.html>
- [8] J.-C. Cuillandre and E.Magnier, private communication, July 2001.
- [9] DIET: See :  
<http://www.cfht.hawaii.edu/Instruments/Imaging/CFH12k/DIET/CFH12K-DIET.html>.
- [10] E. Pécontal, private communication.
- [11] P. Nugent, private communication.
- [12] G. Goldhaber *et al.*, *Astro-ph/0104382*, *ApJ* accepted (2001)
- [13] Phillips, M.M. et al, *Astro-ph/9907052*
- [14] Perlmutter, S., *et al.*, *ApJ* 517, 565 (1999).
- [15] Regnault N., Doctoral Thesis. See :  
[http://www.lal.in2p3.fr/presentation/bibliotheque/publications/2000/regnault\\_thes.ps](http://www.lal.in2p3.fr/presentation/bibliotheque/publications/2000/regnault_thes.ps),  
page 228.
- [16] R. Pello et al., see <http://http://webast.ast.obs-mip.fr/hyperz>

- [17] see <http://www.astrsp-mrs.fr/virmos/>
- [18] see <http://deep.colick.org/>
- [19] A. Coil et al., astro-ph/0009102
- [20] M. Goliath *et al.*, Astro-ph/0104009
- [21] R. Carlberg, Ultra deep Synoptic Survey Time Request, working document for the MSWG, attached to the MSWG report to SAC.

## A Appendix : Simulation of the observing strategy proposed by R. Carlberg

R. Carlberg proposed a different observing strategy [21]:

- The individual exposure times are: g':900 s, r':1800 s, i':3600 s and z':1800 s.
- Observations are scheduled every second day during the dark run (9 observations per run). R. Carlberg proposes an algorithm to decide whether to observe or not, which results in 7 observations per lunation on average.
- One assumes a given field to be observed 5 successive lunations.

We recomputed in that scheme the key figures and tables of what is given above. We did not change the redshift range ( $0.25 < z < 0.95$ ), since the limitation mainly comes from the absence of IR imaging and limited 8-m spectroscopy time.

The peak brightness resolutions of figure 4 become figure A.1. The total statistics of measured SN is now 500 objects.

Table 8 (statistics and resolution) becomes table A.1.

The confidence contours of figure 5 become figure A.2.

The proposed scheme does not improve the resolution on cosmological parameters, making use of all the observing time requested for the Deep Survey : the increase of exposure time with respect to our simulation may be costless. The less favourable point is that observing 5 dark runs in a row instead of 6 costs 25% of the SN Ia statistics at  $z=0.9$ . A real benefit of this scheme is that it is safer from the point of view of systematics than the one we sketched. Finally, if the intrinsic random dispersion of SN Ia decreases as we better understand them, the proposed deeper exposures in i' will actually sharpen distance and cosmological parameters estimates.

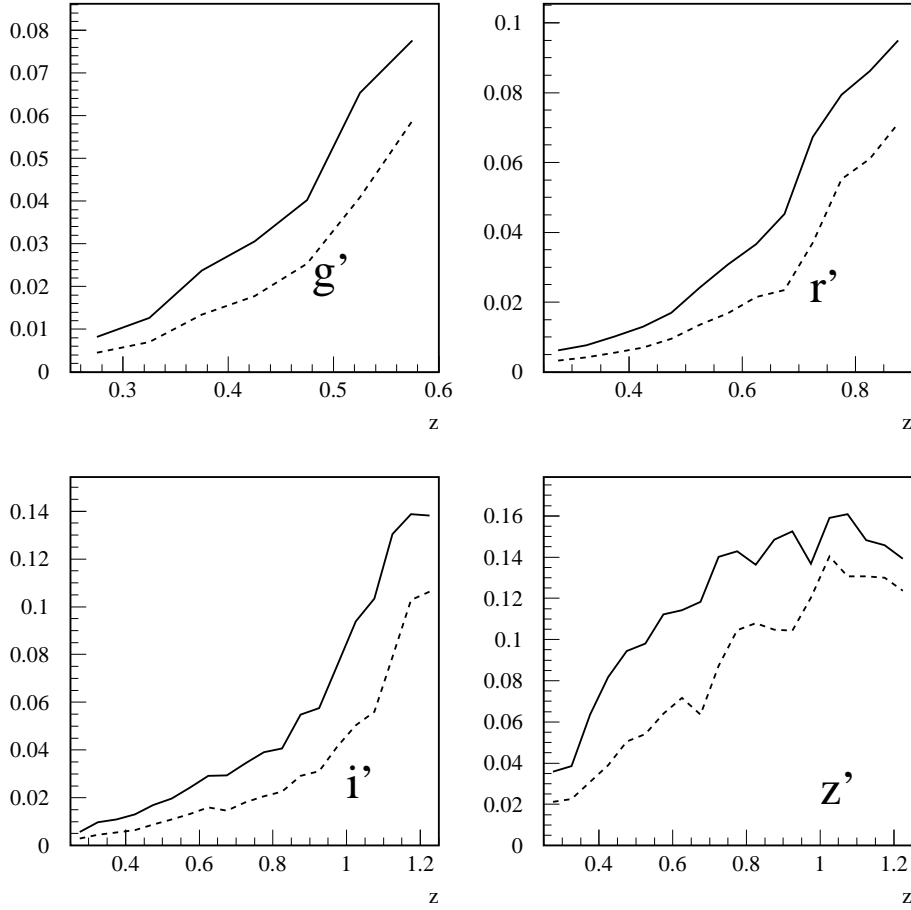


Fig. A.1. *r.m.s* of fitted peak magnitude, corrected for stretch (full line) and uncorrected (dashed line). The assumed exposure times are 900 s in  $g'$ , 1800 s in  $r'$ , 3600 s in  $i'$  and 1800 s in  $z'$ . Both observing times and observing dates vary with respect to fig.4.

Redshift	1 year statistics	$\sigma_{peak}$	$\sigma_{int}$	$\sigma_{tot}$	$\sigma_{color}$	$\sigma_{color}\sqrt{N}$
0.3	7	0.01	0.15	0.15	0.01	-
0.4	10	0.02	0.15	0.15	0.012	-
0.5	13	0.02	0.15	0.15	0.014	-
0.6	15	0.03	0.15	0.153	0.02	-
0.7	16	0.03	0.15	0.153	0.06	0.015
0.8	18	0.04	0.15	0.155	0.09	0.025
0.9	18	0.05	0.15	0.158	0.10	0.030

Table A.1

*Resolutions of stretch corrected peak brightness and color as a function of redshift. The statistics is for 4 fields (1 sq degree each) observed (each) 5 month in a row once. The total statistics is 97 objects.  $\sigma_{peak}$  is the resolution of the stretch corrected peak magnitude.  $\sigma_{int}$  is the intrinsic scatter of SN Ia (after stretch correction).  $\sigma_{tot}$  sums the two previous ones.  $\sigma_{color}$  is the precision of the color measurement. The last column gives the precision on the average color of a 0.1 redshift bin. Up to  $z=0.6$ , the color can be accurately measured on an event per event basis.*

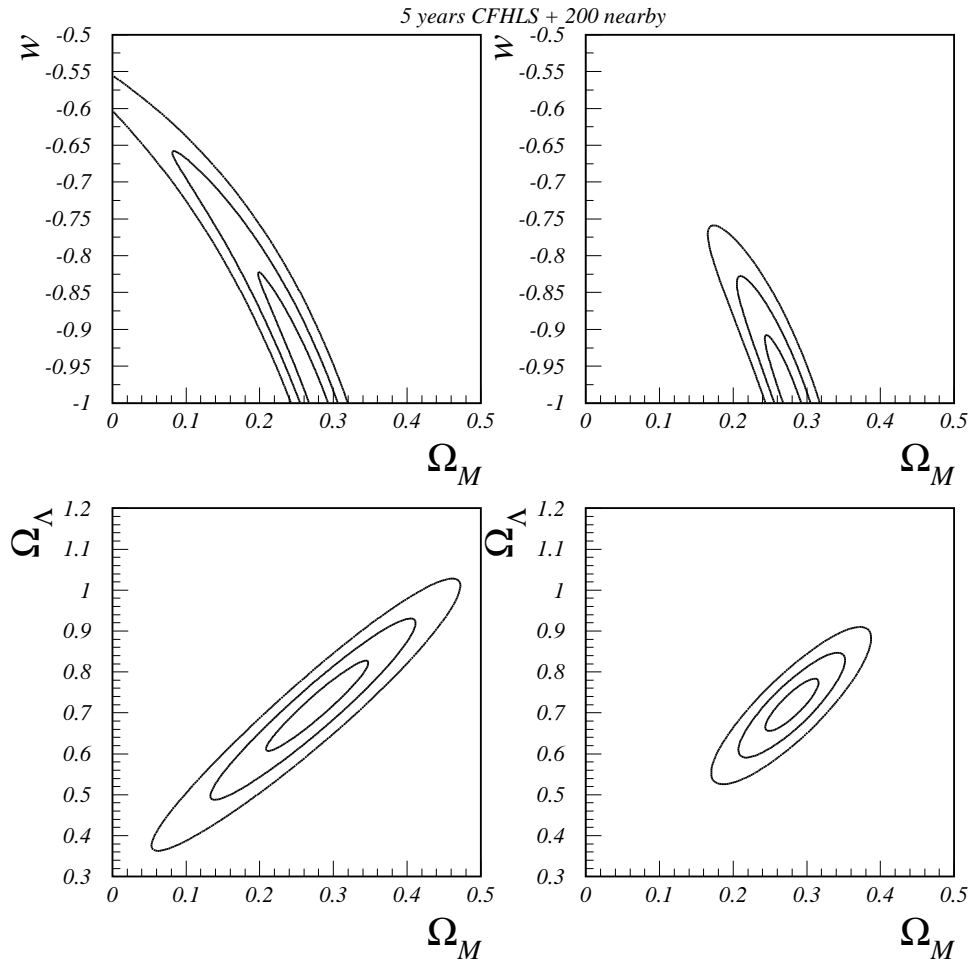


Fig. A.2. One, two and three  $\sigma$  contours (39 ,86 and 99 % CL)for the  $(\Omega_M, w)$  (top) and  $(\Omega_M, \Omega_\Lambda)$  cases for the whole CFHLS statistics + 200 nearby objects. The assumed values for the cosmological parameters are  $\Omega_M = 0.28$ ,  $\Omega_\Lambda = 0.72$  and  $w = -1$ . The plots on the right add a gaussian prior of  $\Omega_M$  with  $\sigma=0.03$  (i.e  $\sim 10\%$ ).